arXiv:1607.04724v2 [cond-mat.dis-nn] 30 Nov 2016

The metastable minima of the Heisenberg spin glass in a random magnetic field

Auditya Sharma,[1] Joonhyun Yeo,[2] and M. A. Moore[3]

[1] *Department of Physics, Indian Institute of Science Education and Research, Bhopal, India*
[2] *Department of Physics, Konkuk University, Seoul 143-701, Korea*
[3] *School of Physics and Astronomy, University of Manchester, Manchester M13 9PL, UK*

We have studied zero temperature metastable minima in classical m-vector component spin glasses in the presence of m-component random fields for two models, the Sherrington Kirkpatrick (SK) model and the Viana Bray (VB) model. For the SK model we have calculated analytically its complexity (the log of the number of minima) for both the annealed case where one averages the number of minima before taking the log and the quenched case where one averages the complexity itself, both for fields above and below the de Almeida Thouless (AT) field, which is finite for $m > 2$. We have done numerical quenches starting from a random initial state (infinite temperature state) by putting spins parallel to their local fields until there is no further decrease of the energy and found that in zero field it always produces minima which have zero overlap with each other. For the $m = 2$ and $m = 3$ cases in the SK model the final energy reached in the quench is very close to the energy E_c at which the overlap of the states would acquire replica symmetry breaking features. These minima have marginal stability and will have long-range correlations between them. In the SK limit we have analytically studied the density of states $\rho(\lambda)$ of the Hessian matrix in the annealed approximation. Despite the fact that in the presence of a random field there are no continuous symmetries, the spectrum extends down to zero with the usual $\sqrt{\lambda}$ form for the density of states for fields below the AT field. However, when the random field is larger than the AT field, there is a gap in the spectrum which closes up as the AT field is approached. The VB model behaves differently and seems rather similar to studies of the three dimensional Heisenberg spin glass in a random vector field.

I. INTRODUCTION

In recent years there has been a resurgence of interest in the properties of metastable states, due mostly to the studies of the jammed states of hard sphere systems; see for reviews Refs. 1 and 2. There are many topics to study, including for example the spectrum of small perturbations around the metastable state, i.e. the phonon excitations and the existence of a boson peak, and whether the Edwards hypothesis works for these states. In this paper we shall study some of these topics in the context of classical Heisenberg spin glasses both in the presence and absence of a random magnetic field. Here the metastable states which we study are just the minima of the Hamiltonian, and so are well-defined outside the mean-field limit. It has been known for some time that there are strong connections between spin glasses and structural glasses [3–5]. It has been argued in very recent work [6] that the study of the excitations in classical Heisenberg spin glasses provides the opportunity to contrast with similar phenomenology in amorphous solids [7, 8]. The minima and excitations about the minima in Heisenberg spin glasses have been studied for many years [9–11] but only in the absence of external fields.

In Sec. II we define the models to be studied as special cases of the long-range one - dimensional m-component vector spin glass where the exchange interactions J_{ij} decrease with the distance between the spins at sites i and j as $1/r_{ij}^{\sigma}$. The spin $\mathbf{S}_i$ is an m-component unit vector. $m = 1$ corresponds to the Ising model, $m = 2$ corresponds to the XY model and $m = 3$ corresponds to the Heisenberg model. By tuning the parameter σ, one can have access to the Sherrington-Kirkpatrick (SK) model and on dilution to the Viana-Bray (VB) model, and indeed to a range of universality classes from mean-field-type to short-range type [12], although in this paper only two special cases are studied; the SK model and the Viana-Bray model. We intend to study the cases which correspond to short-range models in a future publication.

In Sec. III we have used numerical methods to learn about the metastable minima of the SK model and the Viana Bray model. Our main procedure for finding the minima is to start from a random configuration of spins and then align each spin with the local field produced by its neighbors and the external random field, if present. The process is continued until all spins are aligned with their local fields. This procedure finds local minima of the Hamiltonian. In the thermodynamic limit, the energy per spin ε of these states reaches a characteristic value, which is the same for almost all realization of the bonds and random external fields, but slightly dependent on the dynamical algorithm used for selecting the spin to be flipped e.g. the "polite" or "greedy" or Glauber dynamics or the sequential algorithm used in the numerical work in this paper [13, 14]. In the context of Ising spin glasses in zero random fields such states were first studied by Parisi [14]. For Ising spins these dynamically generated states are an unrepresentative subset of the totality of the one-spin flip stable metastable states, which in general have a distribution of local fields $p(h)$ with $p(0)$ is finite [15], whereas those generated dynamically are marginally stable and have $p(h) \sim h$, just like that in the true ground state [16]. Furthermore these states have a trivial overlap with each other: $P(q) = \delta(q)$ [14];

there is no sign of replica symmetry breaking amongst them. Presumably to generate states which show this feature one needs to start from initial spin configurations drawn from a realization of the system at a temperature where broken replica symmetry is already present before the quench.

Because the initial state is random, one would also expect for vector spin glasses that the states reached after the quench from infinite temperature would have only a trivial overlap with each other [13] and this is indeed found to be the case in Sec. III A. We have studied the energy which is reached in the quench for both the $m = 2$ and $m = 3$ SK models but for the case of zero applied random field and in both cases it is very close to the energy E_c which marks the boundary above which the minima where spins are parallel to their local fields have trivial overlaps with each other, while below it the minima have overlaps with full broken replica symmetry features [9, 17]. In Ref. 9 the number $N_S(\varepsilon)$ of minima of energy ε was calculated for the case of zero random field in the SK model and in fact it is only for this model and zero field that the value of E_c is available. That is why in Sec. III B only this case was studied numerically. The work in Sec. IV was the start of an attempt to have the same information in the presence of random vector fields.

The number of minima $N_S(\varepsilon)$ is exponentially large so it is useful to study the complexity defined as $g(\varepsilon) = \ln N_S(\varepsilon)/N$, where N is the number of spins in the system. Despite the fact that minima exist over a large range of values of ε a quench by a particular algorithm seems to reach just the minima which have a characteristic value of ε. What is striking is that this characteristic value is close to the energy E_c at which the minima would no longer have a trivial overlap with each other but would start to acquire replica symmetry breaking features, at least for the $m = 2$ and $m = 3$ SK models in zero field. The states reached in the quenches are usually described as being marginally stable [18]. The coincidence of the energy obtained in the numerical quenches with the analytically calculated E_c suggests that long-range correlations normally associated with a continuous transition will also be found for the quenched minima since such features are present in the analytical work at E_c [17]. In the Ising case the field distribution $p(h)$ produced in the quench is very different from that assumed when determining E_c, and the quenched state energy at ≈ -0.73 was so far below from the Ising value of $E_c = -0.672$ that the connection of its marginality to the onset of broken replica symmetry has been overlooked. We believe that the identification of the energy E_c reached in the quench with the onset of replica symmetry breaking in the overlaps of the minima is the most important of our results.

In Sec. IV we present our analytical work on the m-component SK model in the presence of an m-component random field. It has been shown that in the mean-field limit [19] that under the application of a random magnetic field, of variance h_r^2, there is a phase transition line in the $h_r - T$ plane, the so-called de Almeida-Thouless (AT) line, across which the critical exponents lie in the Ising AT universality class. Below this line, the ordered phase has full replica symmetry breaking. This ordered phase is similar to the Gardner phase expected in high-dimensional hard sphere systems [1]. In Sec. IV we study the minima of the Heisenberg Hamiltonian in the presence of a random vector field. In the presence of such a field the Hamiltonian no longer has any rotational invariances so one might expect there to be big changes in the excitations about the minimum as there will be no Goldstone modes in the system.

We start Sec. IV by studying the number of local minima $N_S(\varepsilon)$ of the Hamiltonian which have energy per spin of ε. The calculation within the annealed approximation, where one calculates the field and bond averages of $N_S(\varepsilon)$ is just an extension of the earlier calculation of Bray and Moore for zero random field [9]. When the random field $h_r > h_{AT}$, where h_{AT} is the field at which the AT transition occurs, the complexity is zero, but $g(\varepsilon)$ becomes non-zero for $h_r < h_{AT}$. When it is non-zero, it is thought better to average the complexity itself over the random fields and bonds so that one recovers results likely to apply to a typical sample. We have attempted to calculate the quenched complexity g for the SK model in the presence of a random field. The presence of this random field greatly complicates the algebra and the calculations in Sec. IV B and the Appendix really just illustrate the problems that random fields pose when determining the quenched average but do not overcome the algebraic difficulties.

The annealed approximation is much simpler and using it we have calculated the density of states $\rho(\lambda)$ of the Hessian matrix associated with the minimum for the SK model. When $h_r > h_{AT}$ there is a gap λ_0 in the spectrum below which there are no excitations. λ_0 tends to zero as $h_r \to h_{AT}$. For $m \geq 4$, $\rho(\lambda) \sim \sqrt{\lambda - \lambda_0}$ as $\lambda \to \lambda_0$. For $m = 3$ the square root singularity did not occur, much to our surprise. For $h_r < h_{AT}$, the square-root singularity applies for all $m > 2$ with $\lambda_0 = 0$. Thus in the low-field phase, despite the fact that in the presence of the random fields there are no continuous symmetries in the system and hence no Goldstone modes, there are massless modes present. In Sec. V B we present numerical work which shows that even for $h_r < h_{AT}$ when the annealed calculation of the density of states of the SK model cannot be exact, it nevertheless is in good agreement with our numerical data.

We have also calculated in Sec. V A the zero temperature spin glass susceptibility χ_{SG} for $h_r > h_{AT}$ for the SK model and find that for all $m > 2$ it diverges to infinity as $h_r \to h_{AT}$ just as is found at finite temperatures [19].

For the SK model, because the complexity is zero for $h_r > h_{AT}$, the quench produces states sensitive to the existence of an AT field. The quench then goes to a state which is the ground state or at least one very like it. The AT field is a feature of the true equilibrium state of the system, which in our case is the state of lowest

energy. In Sec. V A we have studied a "spin glass susceptibility" obtained from the minima obtained in our numerical quenches and only for the SK model is there evidence for a diverging spin glass susceptibility. For the VB model, there is no sign of any singularity in the spin glass susceptibility defined as an average over the states reached in our quench from infinite temperature, but we cannot make any statement concerning the existence of an AT singularity in the true ground state. This is the problem studied in Ref. 20.

Finally in Sec. VI we summarise our main results and make some suggestions for further research.

II. MODELS

The Hamiltonians studied in this paper are generically of the form

$$\mathcal{H} = -m \sum_{\langle i,j \rangle} J_{ij} \mathbf{S}_i \cdot \mathbf{S}_j - \sqrt{m} \sum_i \mathbf{h}_i \cdot \mathbf{S}_i \,, \qquad (1)$$

where the $\mathbf{S}_i$, $i = 1, 2, \cdots, N$, are classical m-component vector spins of unit length. This form of writing the Hamiltonian allows for easy comparison against a Hamiltonian where the spins are normalized to have length $\sqrt{m}$. We are particularly interested in Heisenberg spins, for which $m = 3$. The magnetic fields h_i^μ, where μ denotes a Cartesian spin component, are chosen to be independent Gaussian random fields, uncorrelated between sites, with zero mean, which satisfy

$$[h_i^\mu h_j^\nu]_{av} = h_r^2 \, \delta_{ij} \, \delta_{\mu\nu} \,. \qquad (2)$$

The notation $[\cdots]_{av}$ indicates an average over the quenched disorder and the magnetic fields.

We shall study two models, the Sherrington-Kirkpatrick (SK) model and the Viana-Bray (VB) model. Both are essentially mean-field models. In the Sherrington-Kirkpatrick model, the bonds J_{ij} couple all pairs of sites and are drawn from a Gaussian distribution with zero mean and the variance $1/(N-1)$.

The Viana-Bray model can be regarded as a special case of a diluted one-dimensional model where the sites are arranged around a ring. The procedure to determine the bonds J_{ij} to get the diluted model is as specified in Refs. 12, 21, and 22. The probability of there being a non-zero interaction between sites (i, j) on the ring falls off with distance as a power-law, and when an interaction does occur, its variance is independent of r_{ij}. The mean number of non-zero bonds from a site is fixed to be z. To generate the set of pairs (i, j) that have an interaction with the desired probability the spin i is chosen randomly, and then j $(\neq i)$ is chosen at distance r_{ij} with probability

$$p_{ij} = \frac{r_{ij}^{-2\sigma}}{\sum_{j\,(j\neq i)} r_{ij}^{-2\sigma}} \,, \qquad (3)$$

where $r_{ij} = \frac{N}{\pi} \sin\left[\frac{\pi}{N}(i-j)\right]$ is the length of the chord between the sites i, j when all the sites are put on a circle. If i and j are already connected, the process is repeated until a pair which has not been connected before is found. The sites i and j are then connected with an interaction picked from a Gaussian interaction whose mean is zero and whose standard deviation is set to $J \equiv 1$. This process is repeated precisely $N_b = zN/2$ times. This procedure automatically gives $J_{ii} = 0$. Our work concentrates on the case where the coordination number is fixed at $z = 6$ to mimic the 3-d cubic scenario. The SK limit $(z = N-1, \sigma = 0)$ is a special case of this model, as is the VB model which also has $\sigma = 0$, but the coordination number z has (in this paper) the value 6. The advantage of the one-dimensional long-range model for numerical studies is that by simply tuning the value of σ one can mimic the properties of finite dimensional systems [12, 21, 22] and we have already done some work using this device. However, in this paper we only report on our work on the SK and VB models.

III. NUMERICAL STUDIES OF THE MINIMA OBTAINED BY QUENCHING

In this section we present our numerical studies of the minima of the VB and SK models. We begin by describing how we found the minima numerically. They are basically just quenches from infinite temperature. In Sec. III A we have studied the overlap between the minima and we find that the minima produced have only trivial overlaps with one another. In Sec III B we describe our evidence that the minima of the SK model in zero field have marginal stability as they have an energy per spin close to the energy E_c which marks the energy at which the minima starting to have overlaps showing replica symmetry breaking features.

At zero temperature, the metastable states (minima) which we study are those obtained by aligning every spin along its local field direction, starting off from a random initial state. In the notation used for our numerical work based on Eq. (1) we iterate the equations

$$\mathbf{S}_i^{n+1} = \frac{\mathbf{H}_i^n}{|\mathbf{H}_i^n|}, \qquad (4)$$

where the local fields after the nth iteration, $\mathbf{H}_i^n$, are given by

$$\mathbf{H}_i^n = \sqrt{m}\mathbf{h}_i + m \sum_j J_{ij} \mathbf{S}_j^n. \qquad (5)$$

For a given disorder sample, a random configuration of spins is first created which would be a possible spin configuration at infinite temperature. Starting from the first spin and scanning sequentially all the way up to the N^{th} spin, every spin is aligned to its local field according to Eq. (4), this whole process constituting one sweep. The vector $(\Delta\mathbf{S}_1, \Delta\mathbf{S}_2, \cdots, \Delta\mathbf{S}_N)$ is computed by subtracting the spin configuration before the sweep from the spin configuration generated after the sweep. The quantity

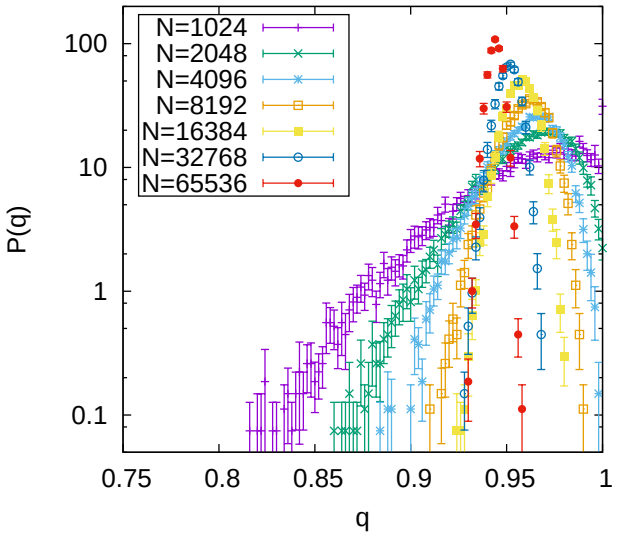

FIG. 1. (Color online) The overlap distribution $P(q)$ for the VB model ($\sigma = 0, z = 6$, $h_r = 0.6$) for the minima generated by the prescription described in the text. $P(q)$ seems to be approaching a delta function as N tends to infinity.

$\eta = \frac{1}{Nm}\sum_{\mu=1}^{m}\sqrt{\sum_{j=1}^{N}(\Delta S_{j\mu})^2}$ is a measure of how close the configurations before and after the sweep are. The spin configurations are iterated over many sweeps until the value of η falls below 0.00001, when the system is deemed to have converged to the metastable state described by Eq. (9), which will be a minimum of the energy at zero temperature. Differing starting configurations usually generate different minima, at least for large systems.

A. Overlap distribution

It is informative to study the overlaps between the various minima. Consider the overlap between two minima A and B defined as

$$q \equiv \frac{1}{N}\sum_i \mathbf{S}_i^A \cdot \mathbf{S}_i^B. \tag{6}$$

Numerically, the following procedure is adopted. A particular realization of the bonds and fields is chosen. Choosing a random initial spin configuration, the above algorithm is implemented and descends to a locally stable state. This generates a metastable spin state that is stored. One then chooses a second initial condition, and the algorithm is applied, which generates a second metastable spin state which is also stored. One repeats this N_{min} times generating in total N_{min} metastable states (some or all of which might be identical). One then overlaps all pairs of these states, so there are $N_{pairs} = N_{min}(N_{min}-1)/2$ overlaps which are all used to make a histogram. The whole process is averaged over N_{samp} samples of disorder. Fig. 1 shows the overlap distribution of the metastable states obtained by the above prescription for the VB model. The figure suggests that in the thermodynamic limit, the distribution of overlaps, $P(q) = \delta(q - q_0(h_r))$. In zero field we have found that $q_0(h_r = 0) = 0$. Since we study only a finite system of N spins, the delta function peak is broadened to a Gaussian centered around q_0 and of width $O(\frac{1}{\sqrt{N}})$. We studied also the SK model, for a range of values for the h_r fields, and the data are consistent with $P(q)$ just having a single peak in the thermodynamic limit. This suggests that the metastable states generated by the procedure of repeatedly putting spins parallel to their local fields starting from a random state always produces minima which have a $P(q)$ of the same type as would be expected for the paramagnetic phase.

Newman and Stein [13] showed that for Ising spins in zero field that when one starts off from an initial state, equivalent to being at infinite temperature, and quenches to zero temperature one always ends up in a state with a trivial $P(q) = \delta(q)$, in agreement, for example with the study of Parisi [14]. Our results for vector spin glasses seem exactly analogous to the Ising results.

B. Marginal stability

In this subsection we shall focus on the Ising, XY ($m = 2$) and Heisenberg ($m = 3$) SK models with zero random field. Parisi found for the Ising case that when starting a quench from infinite temperature, when the spins are just randomly up or down, and putting spins parallel to their local fields according to various algorithms, the final state had an energy per spin $\varepsilon = -0.73$ [14]. In their studies of one-spin flip stable spin glasses in zero field, Bray and Moore [9, 17] found that such states associated with a trivial $P(q) = \delta(q)$ should not exist below a critical energy E_c and for the Ising case $E_c = -0.672$. States with an energy close to -0.73 would be expected to be have a $P(q)$ rather similar to those for full replica symmetry breaking, but those generated in the quench have a trivial $P(q)$. There is no paradox as the states generated in the quench have more than one-spin flip stability [16]. This results in a distribution of local fields behaving at small fields so that $p(h) \sim h$, very different from that expected from the study of the $p(h)$ of one-spin flip stable states [15] for which $p(0)$ is finite, and instead similar to what is found in the true ground state – the state which is stable against flipping an arbitrary number of spins. It is by that means that the theorem of Newman and Stein [13] that in a quench from a random initial state the final $P(q)$ should be trivial is realized, despite the quenched energy being in the region where one would expect the $P(q)$ of one spin flip stable states to be non-trivial. The change in the form of $p(h)$ means that the true E_c is not at -0.672, but instead is at least closer to -0.73.

For the vector SK spin glasses in zero field we have studied the energy reached in a quench from infinite tem-

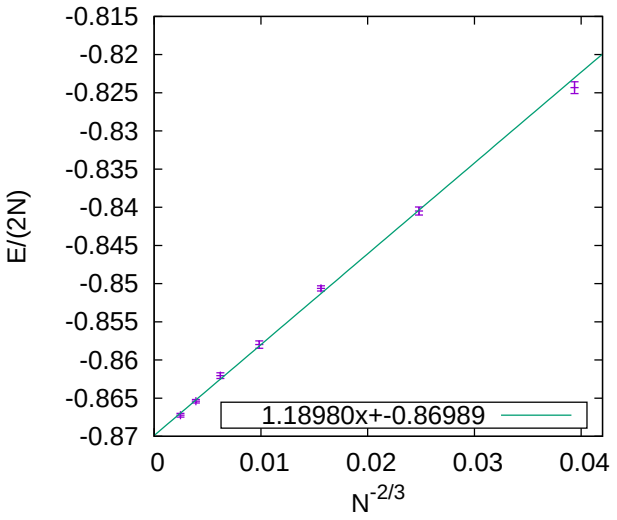

FIG. 2. (Color online) The average energy per site and spin component for the XY SK spin glass model ($m = 2$) with $h_r = 0$ plotted against $1/N^{2/3}$ in order to estimate the infinite system value of the energy obtained from a quench from infinite temperature. For $m = 2$, $E_c = -0.866$ [9].

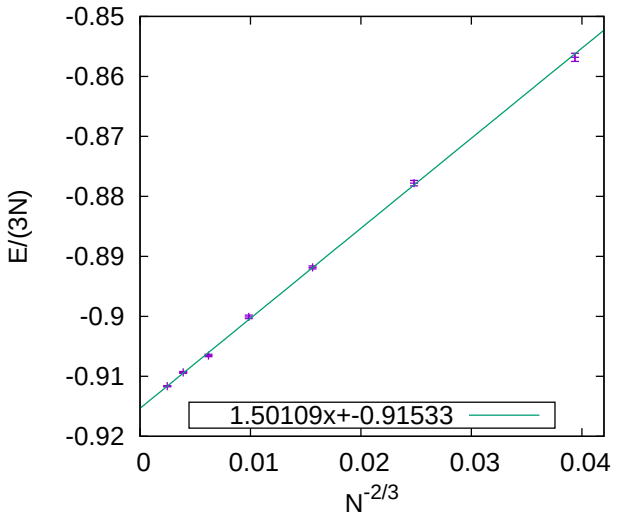

FIG. 3. (Color online) The average energy per site and spin component for the Heisenberg SK spin glass ($m = 3$) with $h_r = 0$ plotted against $1/N^{2/3}$ in order to estimate the infinite system value of the energy obtained from a quench from infinite temperature. For $m = 3$, $E_c = -0.914$ [9].

perature by putting the spins parallel to their local fields. In Figs. 2 and 3 we have plotted our estimates of this energy as a function of $1/N^{2/3}$, the form commonly used for the energy size dependence of the SK model [23, 24]. For $m = 2$, the extrapolated energy per spin component is ≈ -0.870, whereas its $E_c = -0.866$ according to the analysis in Ref. 9; for $m = 3$ the extrapolated energy per spin component is ≈ -0.915 whereas its $E_c = -0.914$ [9]. Minima whose energies lie below the critical energy E_c, are associated with non-trivial (i.e. RSB) form for their $P(q)$, calculated from the overlaps of the minima at the same energy [9, 17]. We found just as for the Ising SK model that the energy reached in the quench varied little when the greedy algorithm was used instead of the sequential algorithm [14].

As the energy of the quenched state is remarkably close to the critical energies calculated by Bray and Moore [9, 17] for $m = 2$ and $m = 3$, this suggests that the state reached in the quench is well-described by the calculations in Ref. 9, whereas for the Ising case the equivalent calculation which enumerates the number of one-spin flip stable states does not give the resulting $p(h)$ of the quenched states with much accuracy and so does not produce an accurate estimate of E_c.

One knows a lot about behavior at E_c at least for Ising spins in zero random field [17]. For states of energy per spin $\varepsilon > E_c$, the annealed and quenched averages agree with each other, but for energies $\varepsilon < E_c$, the two calculations differ. As ε approaches E_c, behavior is as at a critical point, with growing length scales etc. and massless modes [17]. For the Ising case the properties of these modes were discussed in Ref. 17. We intend to return to this topic in a future publication for the case of vector spin glasses.

When one sets an Ising spin parallel to its local field in the course of the quench, spin avalanches may be triggered. If the number of neighbors z is of order N then the avalanches can be on all size scales [25, 26]. Thus the Ising SK model is an example of a system with marginal stability as discussed by Müller and Wyart [18]. It was argued in Ref. 18 that as the quench progresses the system will reach the marginal manifold which separates stable from unstable configurations. As this point is approached the dynamics slows and eventually freezes near the marginal manifold. The VB model with $z = 6$ does not have large scale avalanches [26] and does not have any marginal features; a first study of avalanches in the undiluted one-dimensional long-range models can be found in [25]. While the Ising VB model does not have large scale avalanches, there certainly will be an energy E_c below which the minima will have non-trivial overlaps. What is not clear is whether it is the large avalanches which ensures that the states generated in a quench are close to this energy.

We also do not know what difference the existence of a finite temperature phase might make to the properties of the quenched state. For example, are there features of the quenched states of one and two dimensional Ising spin glasses, where there is no finite temperature spin glass transition, which differ significantly from those of the three dimensional spin glass, where there is a finite temperature phase transition? We also do not know what features might arise if there is a phase transition to a state with full replica symmetry breaking, as opposed to

a state with just replica symmetry.

For systems for which the excitations are not discrete, such as in vector spin glasses, marginality takes a different form, and seems related to the development of negative eigenvalues in the Hessian [18, 27]. Such eigenvalue instabilities might be triggered in a quench where one puts spins parallel to their local fields. On the other hand, one could imagine a steepest descent procedure starting from the initial spin orientation and smoothly proceeding to a minimum. Does that result in a final state whose properties differ from those generated by putting spins parallel to their local fields?

There are many topics which should be studied! We believe that the proximity of the quenched energy to the calculated critical energy E_c, at least for the cases of $m = 2$ and $m = 3$ will provide valuable analytical insights concerning marginal stability. One of our motivations for the analytic work in the next section was to calculate $E_c(h_r)$ in the presence of a non-zero random vector field, but, as we shall see, algebraic difficulties prevented us from achieving this goal. But it would be good to know how general is the result that the energy obtained in a quench coincides with the energy at which the overlaps of the minima display replica symmetry breaking features.

IV. METASTABLE STATES IN THE SK MODEL IN THE PRESENCE OF A RANDOM FIELD

In this section we follow the method of Ref. 9 to study the complexity and Hessian properties of the minima for the SK model but in the presence of a random vector field. We begin by writing down the first steps in the formalism following Ref. 9. In subsection IV A we show that within the annealed approximation, where one averages $N_S(\varepsilon)$ itself over the bonds J_{ij} and the random fields h_i^{ex} analytical progress is fairly straightforward. Fortunately the annealed approximation is also exact for fields $h_r > h_{AT}$. In subsection IV B we describe our attempts to solve the quenched case. We believe that our approach based on replica symmetry assumptions should be good down to its limit of stability which would be at $E_c(h_r)$, but algebraic difficulties prevented us from actually determining $E_c(h_r)$.

We find it convenient to write the Hamiltonian for the m-vector spin glass in an m-component external field as

$$\mathcal{H} = -\frac{m}{2}\sum_{i,j} J_{ij}\boldsymbol{S}_i\cdot\boldsymbol{S}_j - m\sum_i \boldsymbol{h}_i^{\rm ex}\cdot\boldsymbol{S}_i, \qquad (7)$$

where the m-component spins $\boldsymbol{S}_i = \{S_i^\alpha\}$, $(\alpha = 1,\cdots,m,$ $i = 1,\cdots,N)$ have a unit length $S_i = 1$. The interactions J_{ij} are chosen from a Gaussian distribution with zero mean and the variance $1/N$. In this section, for convenience, we use the notation $\boldsymbol{h}_i^{\rm ex} = \boldsymbol{h}_i/\sqrt{m}$ for the random Gaussian external fields with zero mean and the variance

$$\langle h_i^{{\rm ex},\alpha} h_j^{{\rm ex},\beta}\rangle = \frac{h_r^2}{m}\delta_{ij}\delta^{\alpha\beta}. \qquad (8)$$

At zero temperature, the spins are aligned in the direction of the local internal field $\boldsymbol{H}_i$, i.e.

$$\boldsymbol{S}_i = \hat{\boldsymbol{H}}_i \equiv \frac{\boldsymbol{H}_i}{H_i}, \qquad (9)$$

where

$$\boldsymbol{H}_i = \sum_j J_{ij}\boldsymbol{S}_j + \boldsymbol{h}_i^{\rm ex}. \qquad (10)$$

In terms of the local fields, the ground state energy E can be written as

$$E = -\frac{m}{2}\sum_i (H_i + \hat{\boldsymbol{H}}_i\cdot\boldsymbol{h}_i^{\rm ex}). \qquad (11)$$

The number of metastable states with energy ε per site and per spin component is given by

$$\begin{aligned} N_S(\varepsilon) = &\int\prod_{i,\alpha} dH_i^\alpha \int\prod_{i,\alpha} dS_i^\alpha \prod_{i,\alpha}\delta(S_i^\alpha - \hat{H}_i^\alpha) \\ &\times\prod_{i,\alpha}\delta\left(H_i^\alpha - \sum_j J_{ij}S_j^\alpha - h_i^{{\rm ex},\alpha}\right)|\det \mathsf{M}\{J_{ij}\}| \\ &\times\delta\left(Nm\varepsilon + \frac{1}{2}m\sum_i (H_i + \hat{\boldsymbol{H}}_i\cdot\boldsymbol{h}_i^{\rm ex})\right), \end{aligned} \qquad (12)$$

where

$$M_{ij}^{\alpha\beta} = \frac{\partial}{\partial S_j^\beta}(S_i^\alpha - \hat{H}_i^\alpha) = \delta_{ij}\delta^{\alpha\beta} - J_{ij}\frac{P_i^{\alpha\beta}}{H_i} \qquad (13)$$

with $P_i^{\alpha\beta} \equiv \delta^{\alpha\beta} - \hat{H}_i^\alpha\hat{H}_i^\beta$ is the projection matrix.

A. Annealed Approximation

We now calculate the average of $N_S(\varepsilon)$ over the random couplings and the random external fields. As we will see below, the direct evaluation of the quenched average $\langle \ln N_S(\varepsilon)\rangle$ is very complicated. Here we first present the annealed approximation, where we evaluate the annealed complexity $g_A(\varepsilon) = \ln\langle N_S(\varepsilon)\rangle/N$. The whole calculation is very similar to those in Appendix 2 of Ref. 9 except for the part involving the average over the random field. Below we sketch the calculation.

The first delta functions in Eq. (12) can be integrated away. We use the integral representations for the second and third delta functions using the variables x_i^α and u, respectively, along the imaginary axis. The average over the random couplings can be done in an exactly the same way as in Ref. 9. We briefly summarize the results below.

The random couplings appear in the factor

$$\left\langle \exp\Big[-\sum_{i<j} J_{ij}\sum_{i,\alpha}(x_i^\alpha \hat{H}_j^\alpha + x_j^\alpha \hat{H}_i^\alpha)\Big]|\det \mathsf{M}\{J_{ij}\}|\right\rangle_J$$
$$= \exp\Big[\frac{1}{2N}\sum_{i<j}\Big\{\sum_\alpha (x_i^\alpha \hat{H}_j^\alpha + x_j^\alpha \hat{H}_i^\alpha)\Big\}^2\Big] \times \left\langle |\det \mathsf{M}\{J_{ij} - O(\frac{1}{N})\}|\right\rangle_J . \quad (14)$$

After neglecting the $O(1/N)$ term, we evaluate the average of the determinant as [9]

$$\langle|\det \mathsf{M}\{J_{ij}\}|\rangle_J = \exp(\frac{1}{2}Nm\bar{\chi})\prod_i \left(1-\frac{\bar{\chi}}{H_i}\right)^{m-1}, \quad (15)$$

where the susceptibility $\bar{\chi}$ satisfies the self-consistency equation [9]

$$\bar{\chi} = (1-\frac{1}{m})\frac{1}{N}\sum_i \frac{1}{H_i - \bar{\chi}} \quad (16)$$

with the condition $H_i \geq \bar{\chi}$. Using the rotational invariance and the Hubbard-Stratonovich transformation, we can rewrite the exponential factor in front of the determinant as

$$\exp[\frac{1}{2m}\sum_{i,\alpha}(x_i^\alpha)^2] \quad (17)$$
$$\times \int \frac{dv}{(2\pi/Nm)^{1/2}}\ \exp[-\frac{Nm}{2}v^2 + v\sum_{i,\alpha} x_i^\alpha \hat{H}_i^\alpha].$$

In the present case, we have to average over the random field. Collecting the relevant terms, we have

$$\left\langle \exp\Big[-\sum_{i,\alpha}(x_i^\alpha + \frac{1}{2}um\hat{H}_i^\alpha)h_i^{\mathrm{ex},\alpha}\Big]\right\rangle_{\boldsymbol{h}^{\mathrm{ex}}} \quad (18)$$
$$= \exp\Big[\frac{h_r^2}{2m}\sum_{i,\alpha}(x_i^\alpha)^2 + \frac{h_r^2}{2}u\sum_{i,\alpha}x_i^\alpha \hat{H}_i^\alpha + Nm\frac{h_r^2}{8}u^2\Big].$$

All the site indices are now decoupled. We express the condition Eq. (16) using the integral representation of the delta function with the variable λ running along the imaginary axis. Putting all the terms together, we have

$$\langle[N_S(\varepsilon)]\rangle_{J,h^{\mathrm{ex}}} = \int\frac{du}{2\pi i}\int\frac{dv}{\sqrt{2\pi/Nm}}\int d\bar{\chi}\int\frac{d\lambda}{2\pi i}$$
$$\times \exp\Big[Nm\lambda\bar{\chi} + \frac{Nm}{2}\bar{\chi}^2 - Nm\varepsilon u - \frac{Nm}{2}v^2 + Nm\frac{h_r^2}{8}u^2 + N\ln I'\Big], \quad (19)$$

where

$$I' = \int_{H\geq\bar{\chi}}\prod_\alpha dH^\alpha \int\prod_\alpha \frac{dx^\alpha}{2\pi i}\left(1-\frac{\bar{\chi}}{H}\right)^{m-1}$$
$$\times \exp\left[\frac{1+h_r^2}{2m}\sum_\alpha (x^\alpha)^2 + (v+\frac{h_r^2}{2}u)\sum_\alpha x^\alpha \hat{H}^\alpha + \sum_\alpha x^\alpha H^\alpha - (m-1)\lambda(H-\bar{\chi})^{-1} - \frac{m}{2}uH\right] \quad (20)$$

The Gaussian integral over x^α can be done analytically. The integrals in Eq. (19) are evaluated via the saddle point method in the $N\to\infty$ limit. Following the procedure described in Ref. 9, we introduce new variables $\boldsymbol{h} \equiv (H-\bar{\chi})\hat{\boldsymbol{H}}$ and $\Delta = -v - \bar{\chi}$ and use the saddle point condition for $\bar{\chi}$, which is

$$\lambda - \Delta - \frac{u}{2} = 0. \quad (21)$$

We finally have an expression for the annealed complexity $g_A(\varepsilon) \equiv N^{-1}\ln\langle N_S(\varepsilon)\rangle$ as

$$g_A(\varepsilon) = m(-\frac{\Delta^2}{2} - \varepsilon u + \frac{h_r^2}{8}u^2) + \ln I, \quad (22)$$

where

$$I = \left(\frac{m}{2\pi(1+h_r^2)}\right)^{m/2} S_m \int_0^\infty dh\ h^{m-1} \quad (23)$$
$$\times \exp\Big[-\frac{m}{2(1+h_r^2)}(h-\Delta+\frac{h_r^2}{2}u)^2 - \frac{(m-1)}{h}(\Delta+\frac{u}{2}) - \frac{m}{2}uh\Big]$$

with the surface area of the m-dimensional unit sphere $S_m = 2\pi^{m/2}/\Gamma(m/2)$. The parameters Δ and u are determined variationally as $\partial g_A/\partial\Delta = \partial g_A/\partial u = 0$.

We focus on the total number of metastable states, which are obtained by integrating $\exp(Ng_A(\varepsilon))$ over ε, or equivalently by setting $u=0$. Thus we are effectively focussing on the most numerous states, those at the top of the band where $g_A(\varepsilon)$ is largest. In this case, $g_A = -(m/2)\Delta^2 + \ln I_0$, where

$$I_0 = S_m\left(\frac{m}{2\pi(1+h_r^2)}\right)^{m/2}\int_0^\infty dh\ h^{m-1} \times \exp\left[-(m-1)\frac{\Delta}{h} - \frac{m(h-\Delta)^2}{2(1+h_r^2)}\right]. \quad (24)$$

The parameter Δ is determined by the saddle point equation

$$\Delta = \frac{1}{2+h_r^2}\langle h\rangle - \left(1-\frac{1}{m}\right)\left(\frac{1+h_r^2}{2+h_r^2}\right)\left\langle\frac{1}{h}\right\rangle, \quad (25)$$

where the average is calculated with respect to the probability distribution for the internal field given by the integrand of I_0 in Eq. (24). Using $\langle h\rangle = \Delta + \langle h-\Delta\rangle$, we

can rewrite Eq. (24) as

$$\Delta\left[1-\left(1-\frac{1}{m}\right)\left\langle\frac{1}{h^2}\right\rangle\right]=0. \tag{26}$$

For various values of the external field h_r, we solve numerically Eq. (25). For $m=3$, we find that when $h_r > h_{AT}=1$ there is only a trivial solution, $\Delta=0$. (Note that the Almeida-Thouless field h_{AT} at $T=0$ is $h_{AT}=1/\sqrt{m-2}$ [19]). From Eq. (24), we see that in this case $I_0=1$ and the complexity g vanishes above the AT field. For $h_r < h_{AT}$, a nontrivial solution, $\Delta\neq 0$ exists. We find that the values of Δ and g_A increase as the external field h_r decreases from h_{AT}, and approach the known values, 0.170 and 0.00839 at zero external field [9]. For h_r smaller than but very close to h_{AT}, Δ is very small. We may obtain an analytic expression for g_A in this case. By expanding everything in Eq. (26) in powers of Δ, we find for $m=3$ that

$$g_A=\frac{3}{2}(h_{AT}^2-h_r^2)\tilde{\Delta}^2+8\sqrt{\frac{3}{2\pi}}\tilde{\Delta}^3\ln\tilde{\Delta}+O(\tilde{\Delta}^3), \tag{27}$$

where $\tilde{\Delta}=\Delta/\sqrt{1+h_r^2}$. The fact that g_A must be stationary with respect to $\tilde{\Delta}$, enables one to determine how the complexity vanishes as $h_r\to h_{AT}$ and the value of $\tilde{\Delta}$ in this limit.

Using the distribution for the internal field H (or h), we first calculate the spin glass susceptibility $\chi_{SG}\equiv(Nm)^{-1}\mathrm{Tr}\chi^2$ with the susceptibility matrix $\chi=\chi_{ij}^{\alpha\beta}$ [9]. Note that the susceptibility in Eq. (16) is just $\bar{\chi}=(Nm)^{-1}\mathrm{Tr}\chi$. The spin glass susceptibility is given by [9] $\chi_{SG}=(1-\lambda_R)/\lambda_R$, where

$$\lambda_R=1-(1-\frac{1}{m})\frac{1}{N}\sum_i\frac{1}{(H_i-\bar{\chi})^2}. \tag{28}$$

This quantity is exactly the one in the square bracket in Eq. (26). Therefore, since $\Delta\neq 0$ for $h_r < h_{AT}$, λ_R vanishes and consequently χ_{SG} diverges. Above the AT field, there is only a trivial solution $\Delta=0$. In this case the integrals are just Gaussians and we can evaluate explicitly $\frac{1}{N}\sum_i\frac{1}{(H_i-\bar{\chi})^2}$, with the result that $\lambda_R=(h_r^2-1/(m-2))/(1+h_r^2)$, so the spin glass susceptibility as a function of the external random field for $h_r > h_{AT}$ is given by

$$\chi_{SG}=\frac{1+h_{AT}^2}{h_r^2-h_{AT}^2}, \tag{29}$$

provided $h_r > h_{AT}$ and $m>2$. The simple divergence of χ_{SG} as $h_r\to h_{AT}$ is a feature of the SK limit and is not found in the Viana-Bray model at least amongst the quenched states of our numerical studies, see Sec. V A

We now calculate the eigenvalue spectrum of the Hessian matrix A. The calculation closely follows the steps in Ref. 11 for the case of zero external field. We consider (transverse) fluctuations around the $T=0$ solution $\boldsymbol{S}_i^0\equiv\hat{\boldsymbol{H}}_i$ by writing $\boldsymbol{S}_i=\boldsymbol{S}_i^0+\boldsymbol{\epsilon}_i$, where $\boldsymbol{\epsilon}_i=\sum_\alpha\epsilon_i^\alpha\hat{\boldsymbol{e}}_\alpha(i)$ with

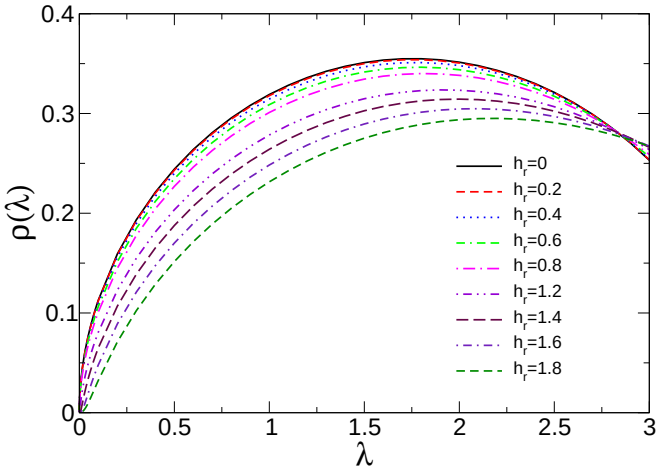

FIG. 4. (Color online) The eigenvalue spectrum of the Hessian at zero temperature for the vector spin glass with $m=3$ in the SK limit.The various lines correspond to different values of h_r, the external random field.

the $(m-1)$ orthonormal vectors $\hat{e}_\alpha(i)$, $\alpha=1,\cdots,m-1$ satisfying $\boldsymbol{S}_i^0\cdot\hat{\boldsymbol{e}}_\alpha(i)=0$. Inserting this into Eq. (7), we have the Hessian matrix as

$$A_{ij}^{\alpha\beta}\equiv\frac{\partial(\mathcal{H}/m)}{\partial\epsilon_i^\alpha\partial\epsilon_j^\beta}=H_i\delta_{ij}\delta^{\alpha\beta}-J_{ij}\hat{\boldsymbol{e}}_\alpha(i)\cdot\hat{\boldsymbol{e}}_\beta(j). \tag{30}$$

The eigenvalue spectrum $\rho(\lambda)$ can be calculated from the resolvent $\mathsf{G}=(\lambda\mathsf{I}-\mathsf{A})^{-1}$ as

$$\rho(\lambda)=\frac{1}{N(m-1)\pi}\mathrm{Im}\ \mathrm{Tr}\mathsf{G}(\lambda-i\delta), \tag{31}$$

where I is the $(m-1)N$-dimensional unit matrix and δ is an infinitesimal positive number. The locator expansion method [28] is used to evaluate $\rho(\lambda)$, which yields the following self-consistent equation for $\bar{G}(\lambda)\equiv((m-1)N)^{-1}\mathrm{Tr}\mathsf{G}(\lambda)$:

$$\bar{G}(\lambda)=\left\langle\frac{1}{\lambda-H-(1-\frac{1}{m})\bar{G}(\lambda)}\right\rangle, \tag{32}$$

where $\langle\ \rangle$ denotes the average over the distribution for h given in the integrand in Eq. (24). Note that $H=h+\bar{\chi}$ and $\bar{\chi}=(1-1/m)\langle 1/h\rangle$ from Eq. (16). We first separate $\bar{G}=\bar{G}'+i\bar{G}''$ into real and imaginary parts and solve Eq. (32) numerically for $\bar{G}'(\lambda)$ and $\bar{G}''(\lambda)$ as a function of λ. The eigenvalue spectrum is just $\rho(\lambda)=\pi^{-1}\bar{G}''(\lambda)$.

As we can see from Figs. 4 and 5, $\rho(\lambda)$ does not change very much as we increase h_r from zero up to $h_{AT}=1$. For the external field larger than the AT field, however, Fig. 5 clearly shows that the eigenvalue spectrum develops a gap. The gap increases with the increasing external field. By directly working on Eq. (32) in the small-λ limit, we find that for small eigenvalues

$$\rho(\lambda)\simeq\frac{1}{\pi(1-1/m)}\frac{1}{\sqrt{s}}\sqrt{\lambda-\lambda_0}, \tag{33}$$

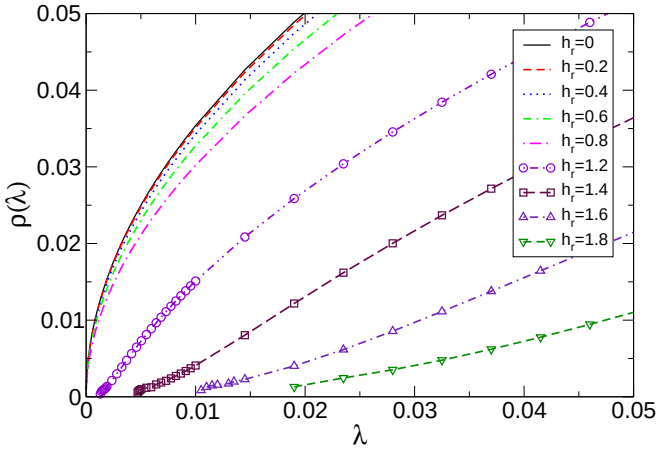

FIG. 5. (Color online) The magnified view of the same figure as Fig. 4 but for the small eigenvalues.

where $s = (1-m^{-1})\langle 1/h^3\rangle$ and $\lambda_0 = \lambda_R^2/4s$ with λ_R defined in Eq. (28). Our numerical solution of the equations for $G(\lambda)$ confirms that there is no gap below h_{AT} which is consistent with the previous observation that λ_R vanishes there. However, the integral by which s is defined diverges for $h_r > h_{AT}$ when $m < 3$ and we no longer see a square root singularity at the band-edge. In the case of $m = 3$ our numerical solution shown in Fig. 5 suggests instead of the square root dependence there is a roughly linear dependence as λ approaches the numerically determined band-edge λ_0, but unfortunately we have not been able to derive its form analytically. Fig. 4 shows that away from λ_0 the density of states is rather as if it had the square root form. As $h_r \to h_{AT}$ this square root form works all the way to zero.

B. Quenched Average

In this subsection, we attempt to evaluate the quenched complexity $g(\varepsilon) = N^{-1}\langle \ln N_S(\varepsilon)\rangle$. The calculations are quite complicated and some of the details are sketched in the Appendix. In order to calculate $\langle \ln N_S(\varepsilon)\rangle$, we consider an average of the replicated quantity $\langle [N_S(\varepsilon)]^n\rangle_{J,h^{\rm ex}}$. We then have an expression similar to Eq. (19), where the integrals are now over replicated variables, u^η, v^η, $\bar\chi^\eta$ and λ^η with the replica indices $\eta, \mu = 1, \cdots, n$. In addition to these, the expression also involves the integrals over the variables carrying off-diagonal replica indices, which are denoted by $A_{\eta\nu}$, $A^*_{\eta\nu}$, $B_{\eta\nu}$ and $B^*_{\eta\nu}$ with $\eta < \nu$. In the absence of external field, it can be shown [9] that $A_{\eta\nu} = A^*_{\eta\nu} = B_{\eta\nu} = B^*_{\eta\nu} = 0$ is always a solution to the saddle point equations. It is shown to be stable for $\varepsilon > E_c$ for the E_c, for which the quenched average coincides with the annealed one. For $h_r \neq 0$, however, we find that this is no longer the case. $A_{\eta\nu} = A^*_{\eta\nu} = B_{\eta\nu} = B^*_{\eta\nu} = 0$ is not a solution to saddle point equations. The saddle point solutions involve nonvanishing off-diagonal variables in replica indices. We find that in general the saddle point equations are too complicated to allow explicit solutions. (See the Appendix for details.)

The quenched average is different from the annealed one for a finite external field when $h_r < h_{AT}$. When $h_r > h_{AT}$ the annealed and quenched averages are identical in every way for the SK model, which has vanishing complexity in this region. We doubt whether the same statement is true for any model such as the Viana-Bray model which has non-zero complexity for $h_r > h_{AT}$. We also do not know for sure whether our replica symmetric solution for $A_{\eta\nu}$ etc. is stable. It is possible that even at $u = 0$ there is a need to go to full replica symmetry breaking. Unfortunately algebraic complexities have prevented us from even finding a solution of the replica symmetric equations, so determining their stability looks very challenging. However, the results of the numerical work reported on the form of $P(q)$ in Sec. III for the Viana-Bray model in a field suggests that the states reached in the quench have replica symmetry.

We look for the saddle points in the replica symmetric form,

$$A_{\eta\nu} = A, \quad A^*_{\eta\nu} = A^*, \quad B_{\eta\nu} = B^*_{\eta\nu} = B,$$
$$u^\eta = u, \quad v^\eta = v, \quad \bar\chi^\eta = \bar\chi, \quad \lambda^\eta = \lambda. \tag{34}$$

After a lengthy calculation (see Appendix), we arrive at the expression for the quenched complexity as follows.

$$\begin{aligned} g(\varepsilon) =& m\Big\{ -\frac{\Delta^2}{2} - \varepsilon u - \frac{A}{2m} + \frac{1}{2}(AA^* + B^2)\Big\} \\ &+ \int \frac{d^m\boldsymbol{w}}{(2\pi)^{m/2}} \int \frac{d^m\boldsymbol{y}}{(2\pi)^{m/2}} \int \frac{d^m\boldsymbol{z} d^m\boldsymbol{z}^*}{(2\pi)^m} \\ &\times \exp[-\frac{1}{2}\sum_\alpha^m (w_\alpha^2 + y_\alpha^2 + z_\alpha z_\alpha^*)]\ \ln K(\boldsymbol{w}, \boldsymbol{y}, \boldsymbol{z}, \boldsymbol{z}^*), \end{aligned} \tag{35}$$

where

$$\begin{aligned} K = \int d^m\boldsymbol{h} \int_{-i\infty}^{i\infty} \frac{d^m\boldsymbol{x}}{2\pi i}\ \exp\Bigg[& \frac{1 - mA^*}{2m}\boldsymbol{x}^2 \\ & + (h - \Delta - B)\boldsymbol{x}\cdot\hat{\boldsymbol{h}} - (m-1)\frac{\Delta + u/2}{h} - \frac{m}{2}uh \\ & + \sqrt{A^* + \frac{h_r^2}{m}}\ \boldsymbol{w}\cdot\boldsymbol{x} + \sqrt{A + \frac{mh_r^2}{4}u^2}\ \boldsymbol{y}\cdot\hat{\boldsymbol{h}} \\ & + \sqrt{\frac{1}{2}(B + \frac{h_r^2}{2}u)}\left(\boldsymbol{z}\cdot\boldsymbol{x} + \boldsymbol{z}^*\cdot\hat{\boldsymbol{h}}\right)\Bigg]. \end{aligned} \tag{36}$$

All the parameters, Δ, A, A^*, B and u are to be determined in a variational way. We found, however, that it is very difficult to solve the saddle point equations and obtain the quenched complexity, even numerically.

For the total number of metastable states, $u = 0$, we can find a simple solution to saddle point equations at $\Delta = A = B = 0$ and $A^* = 1/m$. In this case, $K = 1$ and the complexity g vanishes. This solution must describe the case where $h_r > h_{AT}$ and it is identical to

the annealed average. For the external field h_r just below h_{AT}, Δ, A, B and $C \equiv 1/m - A^*$ are expected to be very small, and we may expand the integrals in Eq. (35) in these variables. We find after a very lengthy calculation that

$$g \simeq \frac{m}{1+h_r^2}(h_{AT}^2 - h_r^2)\Big[\frac{\Delta^2}{2} + \frac{AC}{2} - \frac{B^2}{2}\Big]. \tag{37}$$

Note that from Eq. (A.7), we expect B is pure imaginary. In order to determine how these variables behave near h_{AT}, we need higher order terms. Unfortunately, the complicated nature of these equations, however, has prevented us from going beyond the quadratic orders. It seems natural to expect that the Δ sector is decoupled from the off-diagonal variables, and so will have the same $\Delta^3 \ln \Delta$ behavior as in Eq. (27). But the effort to obtain a full solution is so large that we abandoned further work on it.

V. HESSIAN STUDIES

In this section we write down the Hessian for the $m = 3$ Heisenberg spin glass in a form which is convenient for numerical work. The Hessian is of interest as it describes the nature of the energy of the spin glass in the vicinity of the minima. It is also closely related to the matrices needed to describe the spin waves in the system [9]. We follow the approach used in the paper of Beton and Moore [29] to find the elements of the Hessian matrix T corresponding to directions transverse to each spin subject to the above metastability condition. We first define the site-dependent two-dimensional orthogonal unit vectors $\hat{e}_x(i)$ and $\hat{e}_y(i)$ such that

$$\hat{e}_m(i) \cdot \mathbf{S}_i^0 = 0 \tag{38}$$

$$\hat{e}_m(i) \cdot \hat{e}_n(i) = \delta^{mn}, \tag{39}$$

where $m, n = x, y$ denotes the directions perpendicular to the spin at the ith site, which is deemed in the "z" direction. The linear combinations $\hat{e}_i^{\pm} = \frac{1}{\sqrt{2}}(\hat{e}_x(i) \pm i\hat{e}_y(i))$ turn out to be particularly useful. Expanding $\mathbf{S}_i$ about $\mathbf{S}_i^0$, subject to the condition that the length of the spins remains unchanged yields, upto second-order:

$$\mathbf{S}_i = \mathbf{S}_i^0 + \Gamma_i^x \hat{e}_x(i) + \Gamma_i^y \hat{e}_y(i) - \frac{1}{2}[(\Gamma_i^x)^2 + (\Gamma_i^y)^2]\mathbf{S}_i^0. \tag{40}$$

Equivalently,

$$\mathbf{S}_i = \mathbf{S}_i^0 + Z_i^- \hat{e}_i^+ + Z_i^+ \hat{e}_i^- - Z_i^- Z_i^+ \mathbf{S}_i^0, \tag{41}$$

where $Z_i^{\pm} = \frac{1}{\sqrt{2}}(\Gamma_i^x \pm i\Gamma_i^y)$, and $(Z_i^+)^* = Z_i^-$. Defining the $2N$-dimensional vector

$$|Z\rangle = \begin{pmatrix} Z_i^- \\ Z_i^+ \end{pmatrix}, \tag{42}$$

the change in energy per spin component degree of freedom $\frac{\delta E}{3}$ due to a change in spin orientations $|Z\rangle$, is given by:

$$\frac{\delta E}{3} = \frac{1}{2}\langle Z|T|Z\rangle, \tag{43}$$

where T is the $2N \times 2N$ Hessian matrix given by

$$T = \frac{1}{3}\begin{pmatrix} |\mathbf{H}_i|\delta_{ij} + A_{ij}^* & B_{ij}^* \\ B_{ij} & |\mathbf{H}_i|\delta_{ij} + A_{ij} \end{pmatrix},$$

where the matrix elements are

$$A_{ij} = A_{ji}^* = -3J_{ij}\hat{e}_i^+ \cdot \hat{e}_j^-$$
$$B_{ij} = B_{ji}^* = -3J_{ij}\hat{e}_i^+ \cdot \hat{e}_j^+.$$

Converting to spherical coordinates, the matrix elements are

$$\begin{aligned}
A_{ij}^* &= -\frac{3J_{ij}}{2}[(\cos(\theta_i)\cos(\theta_j)+1)\cos(\phi_i-\phi_j) + i(\cos(\theta_i)+\cos(\theta_j))\sin(\phi_i-\phi_j) + \sin(\theta_i)\sin(\theta_j)] \\
B_{ij}^* &= -\frac{3J_{ij}}{2}[(\cos(\theta_i)\cos(\theta_j)-1)\cos(\phi_i-\phi_j) - i(\cos(\theta_i)-\cos(\theta_j))\sin(\phi_i-\phi_j) + \sin(\theta_i)\sin(\theta_j)] \\
B_{ij} &= -\frac{3J_{ij}}{2}[(\cos(\theta_i)\cos(\theta_j)-1)\cos(\phi_i-\phi_j) + i(\cos(\theta_i)-\cos(\theta_j))\sin(\phi_i-\phi_j) + \sin(\theta_i)\sin(\theta_j)] \\
A_{ij} &= -\frac{3J_{ij}}{2}[(\cos(\theta_i)\cos(\theta_j)+1)\cos(\phi_i-\phi_j) - i(\cos(\theta_i)+\cos(\theta_j))\sin(\phi_i-\phi_j) + \sin(\theta_i)\sin(\theta_j)]
\end{aligned} \tag{44}$$

.

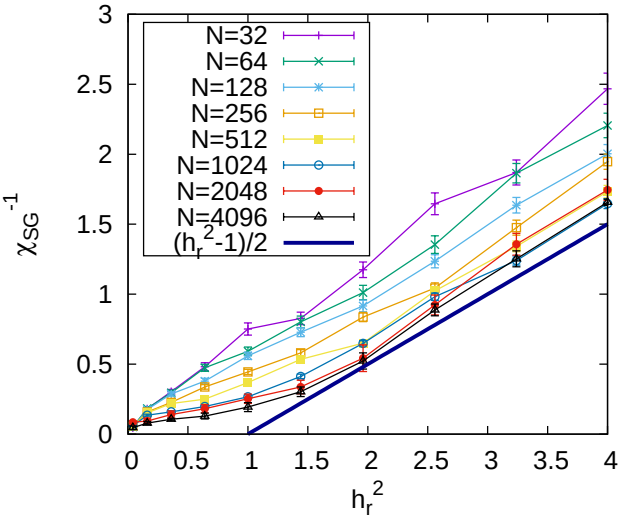

FIG. 6. (Color online) The inverse of the spin glass susceptibility χ_{SG}^{-1} versus h_r^2 for a range of system sizes of the Heisenberg SK model. The analytic curve is the result of Eq. (29). For $h_r \leq 1$, one expects that $\chi_{SG}^{-1} = 0$, but finite size effects make it non-zero.

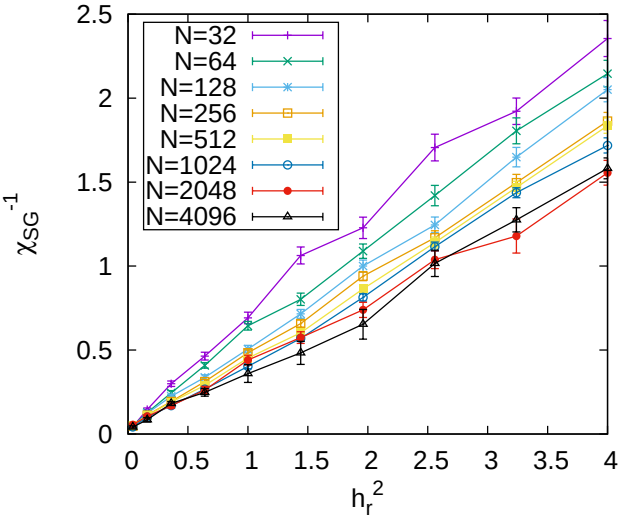

FIG. 7. (Color online) The inverse of the spin glass susceptibility χ_{SG}^{-1} versus h_r^2 for a range of system sizes for the VB model with $z = 6$.

In the next subsection we use the Hessian to numerically calculate the spin glass susceptibility of both the SK model and VB model in a range of random fields for the Heisenberg spin glass.

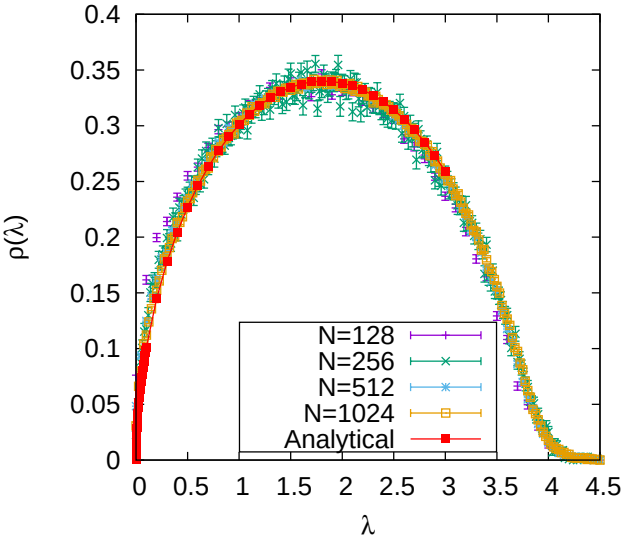

FIG. 8. (Color online) The averaged density of states of the Hessian matrix of the metastable states obtained after a quench to $T = 0$ starting from spins with random orientations i.e. $T = \infty$ for the SK model ($\sigma = 0, z = N - 1$ of the diluted model). Data shown here for the special case of $h_r = 0.8$, for which the system is in the spin glass phase, just below $h_{AT} = 1$. The analytical curve is that calculated from Eqs. (31) and (32)) for metastable states at the top of the band within the annealed approximation. The numerical results are strikingly similar to the analytical results, despite the fact that they refer to Hessians for quite different situations!

A. Spin Glass Susceptibility

The spin glass susceptibility for the metastable states can be computed from the inverse of the Hessian matrix using the relation [9]

$$\chi_{SG} = \frac{1}{N} \mathrm{Tr}\,(T^{-1})^2. \tag{45}$$

For the SK model and $h_r > h_{AT} = 1$, we have calculated χ_{SG} analytically and Fig. 6 shows that our numerical work is approaching the analytical solution, but finite size effects are still very considerable at the sizes we can study. Notice that for the SK model there is (weak) numerical evidence that χ_{SG} diverges below the AT field. For the VB model, the plot of χ_{SG} in Fig. 7 obtained from our metastable states which lie above the true ground state energy provides no evidence that an AT field has much relevance for these states.

B. Density of States

The density of states of the eigenvalues of the Hessian matrix has been obtained numerically for the minima obtained in a quench from infinite temperature to zero temperature. The results have remarkable agreement with

the analytical calculation performed on the Heisenberg SK model as shown in Fig. 8. The analytical calculation itself is not for the same set of metastable states. It applies to the states corresponding to $u = 0$ (i.e. those with the largest complexity within the annealed approximation). In Fig. 8, data are shown for $h_r = 0.8h_{AT}$, where no gap is present. The agreement between the analytical curve which is obtained for the thermodynamic limit, and the data for a $N = 1024$ size system from numerical simulations, is striking. Notice that the $\sqrt{\lambda}$ form predicted from the annealed study (see Sec. IV A) seems to hold as $\lambda \to 0$, despite there being no Goldstone theorem in the presence of a random field to ensure the existence of massless modes.

We have also studied the density of states and quantities like the inverse participation ratios for the quenched state minima in models like the VB model and the one-dimensional long range models. Basically the results seem similar to those reported in Refs. 6 for the three dimensional Heisenberg spin glass model in a random field. But it requires large systems to get accurate results for the density of states at small values of λ and we are leaving these issues to a future publication.

VI. CONCLUSIONS

We believe that the most interesting feature which has turned up in our studies is the discovery for the SK model in zero external fields that the quenched states reached for $m = 2$ and $m = 3$ are quite close to the critical energies E_c at which the overlap of the states would acquire features associated with a $P(q)$ with broken replica symmetry. In the Ising SK model the local fields after the quench are so different from those used in the analytical calculations of E_c that the connection of the quenched state to being just at the edge of the states with broken replica symmetry was not recognized. Thus in systems with marginal stability this means that features normally associated with continuous phase transitions, in particular diverging length scales, could be studied as in Ref. 17.

We have noticed too that the energy of the states reached from the quench have zero overlap with each other. This behavior was predicted for the Ising case in Ref. 13 by Newman and Stein who proved that after a quench from infinite temperature for Ising systems the states which are reached have a characteristic energy and a trivial $P(q)$. It would be good to extend their theorems to vector spin systems both in zero field and also in the presence of random fields.

In Sec. IV we attempted to extend the old calculations of Bray and Moore [9] which were for zero random field to non-zero random fields. For fields $h_r > h_{AT}$ where the complexity is zero, the annealed approximation is exact and we were able to obtain the exact form for the behaviour of the density of states of the Hessian matrix. There was found to be a gap in the spectrum which went to zero in the limit $h_r \to h_{AT}$. When $h_r < h_{AT}$ one needs to study the quenched average in order to get results pertinent to typical minima, but we were not able to overcome the algebraic complexities (see Sec. IV B and the Appendix), although the only difficulty is that of solving the equations which we have obtained. If that could be done then one could investigate the limit of stability of the replica symmetric solution and determine $E_c(h_r)$. Then one could investigate whether a quench in a field h_r takes one to the limit of stability towards full replica symmetry breaking i.e. $E_c(h_r)$, just as we found for $h_r = 0$.

The annealed approximation is tractable but alas it is only an approximation. Nevertheless the studies in Sec. V B shows that it gives good results for the density of states of the Hessian for the SK model for $h_r < h_{AT}$.

The VB model is a mean-field model and one could hope that it too could be understood analytically, but we do not know how this might be achieved. Our numerical studies of the density of states of its Hessian indicates that this is very different from that of the SK model. This is probably because for the SK model all the eigenstates are extended, whereas for the VB model, eigenvectors can also be localized. In fact our results for the VB model are quite similar to those reported for the three dimensional Heisenberg spin glass in a field [6]. There seems to be localized states lying in the gap region, all the way down to $\lambda = 0$. But understanding the VB model analytically is very challenging.

ACKNOWLEDGMENTS

We should like to thank the authors of Ref. 20 for an advance copy of their paper and helpful discussions. One of us (MAM) would like to thank Dan Stein for discussions on quenches in Ising systems. AS acknowledges support from the DST-INSPIRE Faculty Award [DST/INSPIRE/04/2014/002461]. JY was supported by Basic Science Research Program through the National Research Foundation of Korea (NRF) funded by the Ministry of Education (2014R1A1A2053362).

Appendix: The quenched complexity details

We present in this Appendix some of the details of the calculation of the quenched complexity $g(\varepsilon) = N^{-1}\langle \ln N_S(\varepsilon)\rangle$. We first replicate Eq. (12) to obtain

$$[N_S(\varepsilon)]^n = \int \prod_{i,\alpha,\eta} dH_{i\alpha}^{\eta} \int \prod_{i,\alpha,\eta} \frac{dx_{i\alpha}^{\eta}}{2\pi i} \int \prod_{\eta} \frac{du^{\eta}}{2\pi i} \exp\left[\sum_{i,\alpha,\eta} x_{i\alpha}^{\eta} H_{i\alpha}^{\eta} - \sum_{i<j,\alpha,\eta} J_{ij}(x_{i\alpha}^{\eta}\hat{H}_{j\alpha}^{\eta} + x_{j\alpha}^{\eta}\hat{H}_{i\alpha}^{\eta}) - \sum_{i,\alpha,\eta} x_{i\alpha}^{\eta} h_{i\alpha}^{\rm ex}\right]$$
$$\times \prod_{\eta} |\det \mathsf{M}^{\eta}\{J_{ij}\}| \exp\left[-\sum_{\eta} u^{\eta} N m\varepsilon - \sum_{\eta} \frac{1}{2} u^{\eta} m \sum_{i} (H_i^{\eta} + \hat{\boldsymbol{H}}_i^{\eta}\cdot \boldsymbol{h}_i^{\rm ex})\right], \tag{A.1}$$

where $i, j, \ldots = 1, \ldots, N$ are the site indices, $\alpha, \beta, \ldots = 1, \ldots, m$ the vector component indices, and $\eta, \mu, \nu, \ldots = 1, \ldots, n$ replica indices. The average over J_{ij} can be done as in Ref. 9. We have

$$\left\langle \exp\left[-\sum_{i<j} J_{ij} \sum_{i,\alpha} (x_{i\alpha}^{\eta}\hat{H}_{j\alpha}^{\eta} + x_{j\alpha}^{\eta}\hat{H}_{i\alpha}^{\eta})\right] \prod_{\eta} |\det \mathsf{M}^{\eta}\{J_{ij}\}| \right\rangle_J$$
$$= \exp\left[\frac{1}{2N}\sum_{i<j}\left\{\sum_{\alpha,\eta}(x_{i\alpha}^{\eta}\hat{H}_{j\alpha}^{\eta} + x_{j\alpha}^{\eta}\hat{H}_{i\alpha}^{\eta})\right\}^2\right] \left\langle \prod_{\eta} |\det \mathsf{M}^{\eta}\{J_{ij} - O(\frac{1}{N})\}| \right\rangle_J \tag{A.2}$$

After neglecting the $O(1/N)$ term, the determinant can be evaluated to yield the replicated version of Eq. (15). Using the Hubbard-Stratonovich transformation and the rotational invariance, we can write the exponential factor in front of the determinant as

$$\exp\left[\frac{1}{2m}\sum_{i,\alpha,\eta}(x_{i\alpha}^{\eta})^2\right] \int \prod_{\eta} \frac{dv^{\eta}}{(2\pi/Nm)^{1/2}} \exp\left[-\frac{Nm}{2}\sum_{\eta}(v^{\eta})^2 + \sum_{\eta} v^{\eta}\left(\sum_{i,\alpha} x_{i\alpha}^{\eta}\hat{H}_{i\alpha}^{\eta}\right)\right]$$
$$\times \int \prod_{\eta<\nu} \frac{dA_{\eta\nu}dA_{\eta\nu}^*}{(\pi/Nm)} \exp\left[-Nm\sum_{\eta<\nu}|A_{\eta\nu}|^2 + \sum_{\eta<\nu} A_{\eta\nu}^*\left(\sum_{i,\alpha} x_{i\alpha}^{\eta}x_{i\alpha}^{\nu}\right) + \sum_{\eta<\nu} A_{\eta\nu}\left(\sum_{i,\alpha}\hat{H}_{i\alpha}^{\eta}\hat{H}_{i\alpha}^{\nu}\right)\right]$$
$$\times \int \prod_{\eta<\nu} \frac{dB_{\eta\nu}dB_{\eta\nu}^*}{(\pi/Nm)} \exp\left[-Nm\sum_{\eta<\nu}|B_{\eta\nu}|^2 + \sum_{\eta<\nu} B_{\eta\nu}^*\left(\sum_{i,\alpha} x_{i\alpha}^{\eta}\hat{H}_{i\alpha}^{\nu}\right) + \sum_{\eta<\nu} B_{\eta\nu}\left(\sum_{i,\alpha}\hat{H}_{i\alpha}^{\eta}x_{i\alpha}^{\nu}\right)\right] \tag{A.3}$$

The average over the random external field is done as

$$\left\langle \exp\left[-\sum_{i,\alpha,\eta}(x_{i\alpha}^{\eta} + \frac{1}{2}u^{\eta}m\hat{H}_{i\alpha}^{\eta})h_{i\alpha}^{\rm ex}\right]\right\rangle_{\boldsymbol{h}^{\rm ex}} \tag{A.4}$$
$$= \exp\left[\frac{h_r^2}{2m}\sum_{i,\alpha,\eta}(x_{i\alpha}^{\eta})^2 + \frac{h_r^2}{2}\sum_{\eta} u^{\eta}\left(\sum_{i,\alpha} x_{i\alpha}^{\eta}\hat{H}_{i\alpha}^{\eta}\right) + Nm\frac{h_r^2}{8}\sum_{\eta}(u^{\eta})^2\right]$$
$$\times \exp\left[\frac{h_r^2}{m}\sum_{\eta<\nu}\left\{\left(\sum_{i,\alpha} x_{i\alpha}^{\eta}x_{i\alpha}^{\nu}\right) + \frac{m}{2}u^{\nu}\left(\sum_{i,\alpha} x_{i\alpha}^{\eta}\hat{H}_{i\alpha}^{\nu}\right) + \frac{m}{2}u^{\eta}\left(\sum_{i,\alpha}\hat{H}_{i\alpha}^{\eta}x_{i\alpha}^{\nu}\right) + \frac{m^2}{4}u^{\eta}u^{\nu}\left(\sum_{i,\alpha}\hat{H}_{i\alpha}^{\eta}\hat{H}_{i\alpha}^{\nu}\right)\right\}\right].$$

All the site indices are now decoupled. Using the delta function constraint for $\bar{\chi}$, we have

$$\langle [N_S(\varepsilon)]^n\rangle_{J,h^{\rm ex}} = \int \prod_{\eta} du^{\eta} \int \prod_{\eta} dv^{\eta} \int \prod_{\eta} d\bar{\chi}^{\eta} \int \prod_{\eta} d\lambda^{\eta} \int \prod_{\eta<\nu} dA_{\eta\nu}dA_{\eta\nu}^* \int \prod_{\eta<\nu} dB_{\eta\nu}dB_{\eta\nu}^*$$
$$\times \exp\left[Nm\sum_{\eta}\lambda^{\eta}\bar{\chi}^{\eta} + \frac{Nm}{2}\sum_{\eta}(\bar{\chi}^{\eta})^2 - Nm\varepsilon\sum_{\eta} u^{\eta} - \frac{Nm}{2}\sum_{\eta}(v^{\eta})^2 + Nm\frac{h_r^2}{8}\sum_{\eta}(u^{\eta})^2\right.$$
$$\left. - Nm\sum_{\eta<\nu}(|A_{\eta\nu}|^2 + |B_{\eta\nu}|^2) + N\ln I\right], \tag{A.5}$$

where

$$I=\int\prod_{\eta,\alpha}dH_\alpha^\eta\int\prod_{\eta,\alpha}dx_\alpha^\eta\left(1-\frac{\bar\chi^\eta}{H^\eta}\right)^{m-1}$$
$$\times\exp\left[\frac{1+h_r^2}{2m}\sum_{\eta\alpha}(x_\alpha^\eta)^2+\sum_\eta(v^\eta+\frac{h_r^2}{2}u^\eta)\sum_\alpha x_\alpha^\eta\hat H_\alpha^\eta+\sum_{\eta,\alpha}x_\alpha^\eta H_\alpha^\eta-(m-1)\sum_\eta\lambda^\eta(H^\eta-\bar\chi^\eta)^{-1}-\frac{m}{2}\sum_\eta u^\eta H^\eta\right]$$
$$\times\exp\left[\sum_{\eta<\nu}(A_{\eta\nu}^*+\frac{h_r^2}{m})\left(\sum_\alpha x_\alpha^\eta x_\alpha^\nu\right)+\sum_{\eta<\nu}(A_{\eta\nu}+\frac{mh_r^2}{4}u^\eta u^\nu)\left(\sum_\alpha\hat H_\alpha^\eta\hat H_\alpha^\nu\right)\right]$$
$$\times\exp\left[\sum_{\eta<\nu}(B_{\eta\nu}^*+\frac{h_r^2}{2}u^\nu)\left(\sum_\alpha x_\alpha^\eta\hat H_\alpha^\nu\right)+\sum_{\eta<\nu}(B_{\eta\nu}+\frac{h_r^2}{2}u^\eta)\left(\sum_\alpha\hat H_\alpha^\eta x_\alpha^\nu\right)\right]\tag{A.6}$$

The saddle point equation for the off-diagonal variables are given by

$$A_{\eta\nu}=\frac{1}{m}\langle\sum_\alpha x_\alpha^\eta x_\alpha^\nu\rangle,\quad A_{\eta\nu}^*=\frac{1}{m}\langle\sum_\alpha\hat H_\alpha^\eta\hat H_\alpha^\nu\rangle,\quad B_{\eta\nu}=\frac{1}{m}\langle\sum_\alpha x_\alpha^\eta\hat H_\alpha^\nu\rangle,\quad B_{\eta\nu}^*=\frac{1}{m}\langle\sum_\alpha\hat H_\alpha^\eta x_\alpha^\nu\rangle,\tag{A.7}$$

where $\langle\ \rangle$ is calculated with respect to I. We can easily see that when $h_r\neq0$, these averages do not become zero even when all the integration variables carrying off-diagonal replica indices vanish. Therefore $A_{\eta\nu}=A_{\eta\nu}^*=B_{\eta\nu}=B_{\eta\nu}^*=0$ is not a solution of the saddle point equations.

We now study the saddle points in the replica symmetric form,

$$A_{\eta\nu}=A,\quad A_{\eta\nu}^*=A^*,\quad B_{\eta\nu}=B_{\eta\nu}^*=B,\quad u^\eta=u,\quad v^\eta=v,\quad\bar\chi^\eta=\bar\chi,\quad\lambda^\eta=\lambda.\tag{A.8}$$

Then

$$g(\varepsilon)=N^{-1}\langle\ln N_S(\varepsilon)\rangle_{J,h^{\rm ex}}=m\Big\{\lambda\bar\chi+\frac{1}{2}\bar\chi^2-\varepsilon u-\frac{1}{2}v^2+\frac{h_r^2}{8}u^2+\frac{1}{2}(|A|^2+B^2)\Big\}+\lim_{n\to0}[\frac{1}{n}\ln I],\tag{A.9}$$

where

$$I=\int\prod_{\eta,\alpha}dH_\alpha^\eta\int\prod_{\eta,\alpha}dx_\alpha^\eta\left(1-\frac{\bar\chi}{H^\eta}\right)^{m-1}\tag{A.10}$$
$$\times\exp\left[\frac{1+h_r^2}{2m}\sum_{\eta,\alpha}(x_\alpha^\eta)^2+(v+\frac{h_r^2}{2}u)\sum_{\eta,\alpha}x_\alpha^\eta\hat H_\alpha^\eta+\sum_{\eta,\alpha}x_\alpha^\eta H_\alpha^\eta-(m-1)\lambda\sum_\eta(H^\eta-\bar\chi)^{-1}-\frac{m}{2}u\sum_\eta H^\eta\right]$$
$$\times\exp\left[(A^*+\frac{h_r^2}{m})\sum_{\eta<\nu}\sum_\alpha x_\alpha^\eta x_\alpha^\nu+(A+\frac{mh_r^2}{4}u^2)\sum_{\eta<\nu}\sum_\alpha\hat H_\alpha^\eta\hat H_\alpha^\nu\right]$$
$$\times\exp\left[(B+\frac{h_r^2}{2}u)\sum_{\eta<\nu}\left(\sum_\alpha x_\alpha^\eta\hat H_\alpha^\nu+\sum_\alpha\hat H_\alpha^\eta x_\alpha^\nu\right)\right].$$

We now use the Hubbard-Stratonovich transformations on the last three terms in the previous equation using the auxiliary variables, w_α, y_α, z_α and z_α^*, to disentangle the replica indices. Then we can write

$$\int\prod_{\eta,\alpha}dH_\alpha^\eta\int\prod_{\eta,\alpha}dx_\alpha^\eta\sum_\eta(\cdots)=\left[\int\prod_\alpha dH_\alpha\int\prod_\alpha dx_\alpha(\cdots)\right]^n.\tag{A.11}$$

By explicitly evaluating $\lim_{n\to0}n^{-1}\ln I$, we obtain

$$g(\varepsilon)=m\Big\{\lambda\bar\chi+\frac{1}{2}\bar\chi^2-\varepsilon u-\frac{1}{2}v^2-\frac{A}{2m}+\frac{1}{2}(AA^*+B^2)\Big\}$$
$$+\int\prod_\alpha\frac{dw_\alpha}{\sqrt{2\pi}}\int\prod_\alpha\frac{dy_\alpha}{\sqrt{2\pi}}\int\prod_\alpha\frac{dz_\alpha dz_\alpha^*}{2\pi}\ \exp[-\frac{1}{2}\sum_\alpha(w_\alpha^2+y_\alpha^2+|z_\alpha|^2)]\ \ln J,\tag{A.12}$$

where

$$J = \int \prod_\alpha dH_\alpha \int_{-i\infty}^{i\infty} \prod_\alpha \frac{dx_\alpha}{2\pi i} \left(1 - \frac{\bar\chi}{H}\right)^{m-1} \tag{A.13}$$
$$\times \exp\left[\frac{1-mA^*}{2m}\sum_\alpha (x_\alpha)^2 + (v-B)\sum_\alpha x_\alpha \hat H_\alpha + \sum_\alpha x_\alpha H_\alpha - (m-1)\lambda(H-\bar\chi)^{-1} - \frac{m}{2}uH\right]$$
$$\times \exp\left[\sqrt{A^* + \frac{h_r^2}{m}}\sum_\alpha w_\alpha x_\alpha + \sqrt{A + \frac{mh_r^2}{4}u^2}\sum_\alpha y_\alpha \hat H_\alpha + \sqrt{\frac{1}{2}(B + \frac{h_r^2}{2}u)}\sum_\alpha \left(z_\alpha x_\alpha + z_\alpha^* \hat H_\alpha\right)\right].$$

Now we change the integration variable in J from $\boldsymbol{H}$ to $\boldsymbol{h} \equiv \boldsymbol{H} - \bar\chi \hat{\boldsymbol{H}} = (H - \bar\chi)\hat{\boldsymbol{H}}$. The lower limit of the integral for $\boldsymbol{h}$ now becomes 0 and the Jacobian exactly cancels the factor of $(1 - \bar\chi/H)^{m-1}$. Let us also use the new variable Δ, where $v = -\chi - \Delta$ so that $H + v = h - \Delta$. Extremizing with respect to χ in $g(\varepsilon)$ yields $\lambda - \Delta - u/2 = 0$. We finally have

$$g(\varepsilon) = m\Big\{ -\frac{\Delta^2}{2} - \varepsilon u - \frac{A}{2m} + \frac{1}{2}(AA^* + B^2)\Big\}$$
$$+ \int \frac{d^m\boldsymbol{w}}{(2\pi)^{m/2}} \int \frac{d^m\boldsymbol{y}}{(2\pi)^{m/2}} \int \frac{d^m\boldsymbol{z} d^m\boldsymbol{z}^*}{(2\pi)^m}\ \exp[-\frac{1}{2}\sum_\alpha (w_\alpha^2 + y_\alpha^2 + |z_\alpha|^2)]\ \ln K(\boldsymbol{w}, \boldsymbol{y}, \boldsymbol{z}, \boldsymbol{z}^*), \tag{A.14}$$

where

$$K = \int d^m\boldsymbol{h} \int_{-i\infty}^{i\infty} \frac{d^m\boldsymbol{x}}{2\pi i}\ \exp\left[\frac{1-mA^*}{2m}\boldsymbol{x}^2 + (h - \Delta - B)\boldsymbol{x}\cdot\hat{\boldsymbol{h}} - (m-1)\frac{\Delta + u/2}{h} - \frac{m}{2}uh\right]$$
$$\times \exp\left[\sqrt{A^* + \frac{h_r^2}{m}}\ \boldsymbol{w}\cdot\boldsymbol{x} + \sqrt{A + \frac{mh_r^2}{4}u^2}\ \boldsymbol{y}\cdot\hat{\boldsymbol{h}} + \sqrt{\frac{1}{2}(B + \frac{h_r^2}{2}u)}\left(\boldsymbol{z}\cdot\boldsymbol{x} + \boldsymbol{z}^*\cdot\hat{\boldsymbol{h}}\right)\right]. \tag{A.15}$$

[1] P. Charbonneau, J. Kurchan, G. Parisi, P. Urbani, and F. Zamponi, eprint arXiv:cond-mat/1605.03008 (2016).
[2] A. Baule, F. Morone, H. J. Herrmann, and H. A. Makse, e-print arXiv:cond-mat/1602.04369 (2016).
[3] M. Tarzia and M. A. Moore, Phys. Rev. E **75**, 031502 (2007).
[4] C. J. Fullerton and M. A. Moore, eprint arXiv:cond-mat/1304.4420 (2013).
[5] M. A. Moore and J. Yeo, Phys. Rev. Lett. **96**, 095701 (2006).
[6] M. Baity-Jesi, V. Martín-Mayor, G. Parisi, and S. Perez-Gaviro, Physical Review Letters **115**, 267205 (2015).
[7] M. Wyart, S. R. Nagel, and T. A. Witten, EPL (Europhysics Letters) **72**, 486 (2005).
[8] P. Charbonneau, E. I. Corwin, G. Parisi, A. Poncet, and F. Zamponi, ArXiv e-prints (2015), arXiv:1512.09100 [cond-mat.dis-nn].
[9] A. J. Bray and M. A. Moore, Journal of Physics C: Solid State Physics **14**, 2629 (1981).
[10] J. Yeo and M. A. Moore, Phys. Rev. Lett. **93**, 077201 (2004).
[11] A. J. Bray and M. A. Moore, Journal of Physics C: Solid State Physics **15**, 2417 (1982).
[12] L. Leuzzi, G. Parisi, F. Ricci-Tersenghi, and J. Ruiz-Lorenzo, Physical Review Letters **101**, 107203 (2008).
[13] C. M. Newman and D. L. Stein, Phys. Rev. E **60**, 5244 (1999).
[14] G. Parisi, eprint arXiv:cond-mat/9501045 (1995).
[15] S. A. Roberts, Journal of Physics C: Solid State Physics **14**, 3015 (19
[16] L. Yan, M. Baity-Jesi, M. Müller, and M. Wyart, Phys. Rev. Lett. **114**, 247208 (2015).
[17] A. J. Bray and M. A. Moore, Journal of Physics C: Solid State Physics **14**, 1313 (1981).
[18] M. Müller and M. Wyart, Annual Review of Condensed Matter Physics **6**, 177 (2015).
[19] A. Sharma and A. P. Young, Physical Review E **81**, 061115 (2010).
[20] C. Lupo, G. Parisi, and F. Ricci-Tersenghi, private communication and to be published (2016).
[21] A. Sharma and A. P. Young, Physical Review B **83**, 214405 (2011).
[22] A. Sharma and A. P. Young, Physical Review B **84**, 014428 (2011).
[23] S. Boettcher, Eur. Phys. J. B **31**, 29 (2003).
[24] T. Aspelmeier, A. Billoire, E. Marinari, and M. A. Moore, Journal of Physics A: Mathematical and Theoretical **41**, 324008 (2008).
[25] B. Gonçalves and S. Boettcher, Journal of Statistical Mechanics: Theory and Experiment **2008**, P01003 (2008).
[26] J. C. Andresen, Z. Zhu, R. S. Andrist, H. G. Katzgraber, V. Dobrosavljević, and G. T. Zimanyi, Phys. Rev. Lett.

111, 097203 (2013).
[27] A. Sharma, A. Andreanov, and M. Müller, Physical Review E **90**, 042103 (2014).
[28] A. J. Bray and M. A. Moore, Journal of Physics C: Solid State Physics **12**, L441 (1979).
[29] P. H. Beton and M. A. Moore, Journal of Physics C: Solid State Physics **17**, 2157 (1984).